ОБЪЕДИНЕННЫЙ
ИНСТИТУТ
ЯДЕРНЫХ
ИССЛЕДОВАНИЙ
ДУБНА

E7 - 6970

A.G.Artukh, G.F.Gridnev, V.L.Mikheev,
V.V.Volkov, J.Wilczynski

TRANSFER REACTIONS IN THE INTERACTION OF ^{40}Ar WITH ^{232}Th

1973

ЛАБОРАТОРИЯ ЯДЕРНЫХ РЕАКЦИЙ

E7 - 6970

A.G.Artukh, G.F.Gridnev, V.L.Mikheev,
V.V.Volkov, J.Wilczynski*

TRANSFER REACTIONS IN THE INTERACTION OF ^{40}Ar WITH ^{232}Th

Submitted *to Nuclear Physics*

* On leave from the Institute
of Nuclear Physics, Crakow, Poland.

Summary

Transfer reactions in the bombardment of ^{232}Th target with 297 and 388 MeV ^{40}Ar ions have been studied. The energy spectra, angular distributions and the cross sections for the formation of products, having atomic numbers $5 \leq Z \leq 20$, have been measured. In the energy spectra of the reaction products broad peaks, having energies in the vicinity of the output Coulomb barrier height, have been observed along with the quasielastic ones. The dependence of the partial angular distribution of the light products on the reaction Q-value has been determined. The observed partial angular distributions have been analysed by applying the Strutinsky model. The total cross sections of light product formation have been found to be 1100 mb and 2400 mb for the ^{40}Ar energies $E = 297$ MeV and $E = 388$ MeV, which give the values of the critical angular momentum of $102\hbar$ and $94\hbar$ respectively for the two cases.

1. Introduction

Nuclear reactions induced by the heavy ions such as Ar, Zn, Kr, Xe [1-4], have become of great importance in the recent years. Reactions induced by such ions may result in the synthesis of superheavy elements in a new stability region. Transfer reactions in the bombardment of heavy nuclei by ^{40}Ar ions proved to be an effective means for obtaining new neutron-rich isotopes of light elements [5]. Therefore, the study of the peculiarities of the mechanism of nuclear reactions with heavy ions and the yield of various products, both light and heavy, becomes still more significant.

The majority of investigations of direct heavy ion reactions on heavy nuclei have been performed by radiochemical separation of reaction products [1,6-8]. However, this method does not allow the detection of stable products as well as radioactive products having either very short or very long half-lives. It is even more difficult to measure their energy spectra. The combination of the magnetic analysis and the $\Delta E, E$ methods [9] is free from such disadvantages and makes it possible to identify unambiguously the light products of reactions over a wide range of A and Z. However, this technique used for measuring the angular and energy distributions of many reaction products requires much accelerator time. The $\Delta E, E$ method is more efficient, though it involves some difficulties in isotope separation, especially with $Z > 8$ ref. [10,11].

The study of some general features of the direct reaction, such as the total cross sections and the cross sections for the production of some element, does not require the knowledge of

the mass number of products when reliable Z separation has been done. Some reaction properties such as the angular distributions of neighbouring isotopes differ slightly [6,8,12]. Earlier, in bombarding ^{232}Th with ^{40}Ar ions we have found that the major contribution (of 75-85%) to the formation cross section of elements at an angle of 40^0 comes from 3-4 neighbouring isotopes [5]. Angular and energy distributions for the given element may be expected to be close to those of separate isotopes which form the major part of the element produced.

The present investigation was aimed at measuring the cross sections, angular and energy distributions of the light reaction products formed in the bombardment of ^{232}Th by 297 MeV and 388 MeV ^{40}Ar ions using the ''element'' approach.

2. Experimental Procedure

The $^{40}Ar\ (+7)$ and $^{40}Ar(+8)$ external beams of 2×10^{11} and 6×10^{10} particles/sec and energies 297MeV and 388 MeV, respectively, from the 310-cm Dubna cyclotron were used for bombarding a metallic ^{232}Th target.

Reaction products were detected by a telescope consisting of two silicon surface-barrier detectors: ΔE detector 27 μm thick and the total absorption detector (E). The aperture was defined by a diaphragm of 5 mm in diameter placed in front of the ΔE detector at 250 mm from the target. The angular resolution of the telescope was found to be not worse than $\pm 1.5^0$ with the beam spot dimension of 6×6 mm^2 and the angular divergence of the beam less than $\pm 0.5^0$. The relative accuracy of the telescope location was $\pm 0.1^0$. A thin gold foil, 130 μg/cm^2 thick, protected the detectors from the slow electron flux emitted by the bombarded target. Pulses from both the detectors were fed into a converter for a two-parameter pulse height analysis. The two-dimensional ΔE, $(E-\Delta E)$ spectrum was recorded in two 4096-channel analysers operating in the $256\ (\Delta E) \times 32\ (E - \Delta E)$ channel mode. Product yields at various angles were normalized with respect to the number of elastically scattered ^{40}Ar ions detected in a monitor solid state detector which was placed at an angle of 30^0 to the beam.

3. Experimental Results

3.1. Energy Spectra

Since the energy losses of detected ions in a target were considerable, it was assumed that nuclear reactions occur in a middle plane of the target. The energy losses of reaction products in a target were determined by comparing the energy of ^{40}Ar ions elastically scattered from a ^{197}Au target of thickness 130 μg/cm^2 and the ^{232}Th target used in our experiment. By employing dE/dx tables for heavy ions (in Au and U) of Northcliffe and Shilling [13] it was found that our ^{232}Th target is equivalent to 3.9 mg/cm^2 of uranium. This value together with the data on dE/dx was later used to determine the energy losses of products in the target. Earlier, in bombarding ^{232}Th by ^{40}Ar ions of energy 290 MeV it was established that at an angle of 40^0 the following isotopes: ^{19}O, ^{21}F, ^{24}Ne, ^{26}Na, ^{28}Mg, ^{30}Al, ^{33}Si, ^{35}P, ^{36}S, ^{39}Cl, ^{40}Ar, ^{42}K and ^{44}Ca [5] have the maximum yield. All the calculations were made for the mass numbers of the above isotopes. It is worth noting that these isotopes are obtained with the total number of transferred nucleons close to twice the number of transferred protons. Such a ratio has been obtained by the authors for the $^{232}Th + {}^{22}Ne$ reaction [14].

The absolute values of product yields were calculated from the ratio of reaction product yields and elastically scattered ^{40}Ar at angles of $20\text{-}30^0$ for 297 MeV and $20\text{-}25^0$ for 388 MeV. It is possible to consider the $\sigma_{el}/\sigma_{Ruth}$ ratio to be unity for these angles [15].

Figs. 1 and 2 show the energy spectra of different products from Mg to Ca in the lab. system, the ^{40}Ar energy in the middle plane of the target being $E_0 = 288$ MeV. The energy spectra of lighter products and all the products at larger detection angles are not given since the low yield of these products does not make it possible to plot them with sufficient accuracy. However an evaluation of their formation cross section was made and this was used in plotting their angular distributions.

Figs. 3,4 and 5 show the energy spectra of different products from O to Ca at the ^{40}Ar ion energy $E_0 = 379$ MeV. Some properties characteristic of the energy spectra are worth noting.

The spectra cover rather a wide energy region: 80-120 MeV for $E_0 = 288$ MeV and 110-220 MeV for $E_0 = 379$ MeV. A comparison of the energy spectra of elements and their isotopes emitted at the angle of 40^0 in irradiation of a ^{232}Th target

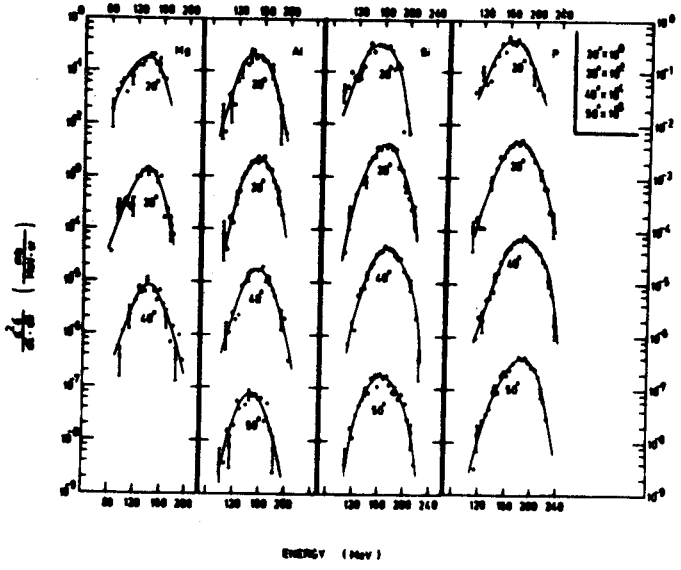

Fig. 1. The laboratory energy spectra of light products obtained in the bombardment of ^{232}Th with 297 MeV ^{40}Ar ions. The product energies have been recalculated for energies in the middle plane of the target. The curves have been drawn through experimental points. All the curves and points for each detection angle have been multiplied by the coefficients in the top right-hand side of the figure.

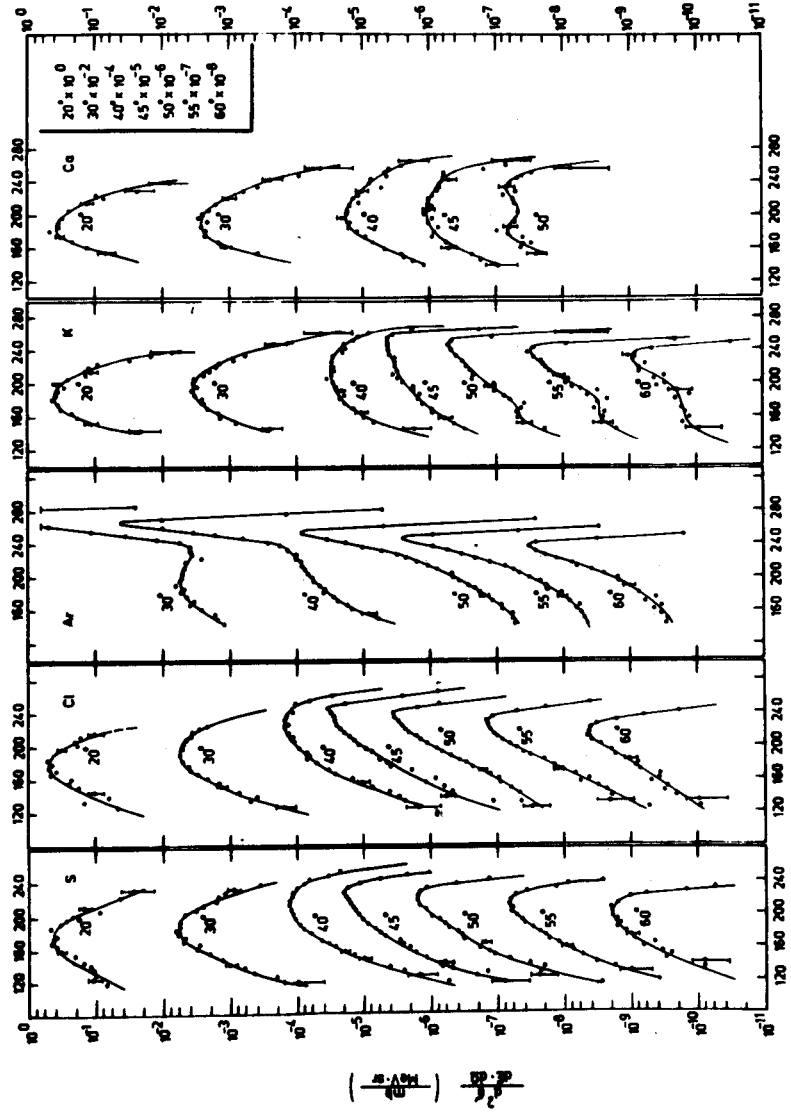

Fig. 2. See caption to Fig. 1.

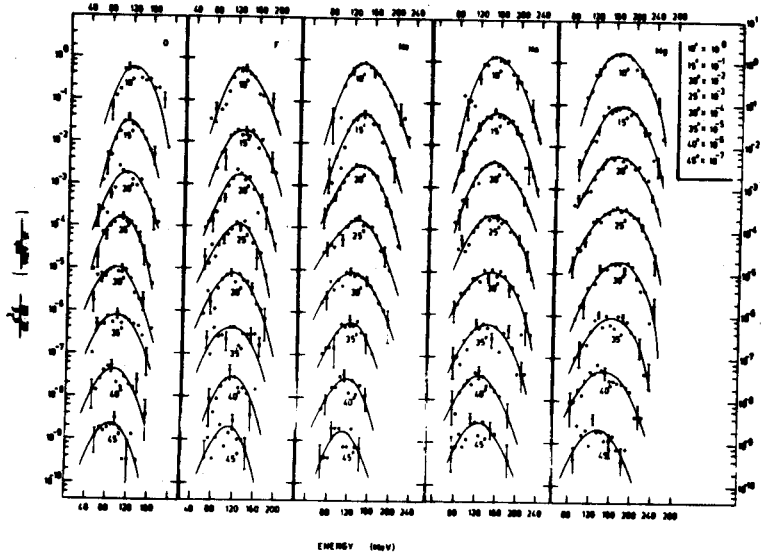

Fig. 3. The laborarory energy spectra of light products obtained in the bombardment of ^{232}Th with **388 MeV** ^{40}Ar ions. The product energies have been recalculated for the energies in the middle plane of the target. The curves have been drawn through experimental points. All the curves and points for each detection angle have been multipled by the coefficients shown in the top right-hand side of the figure.

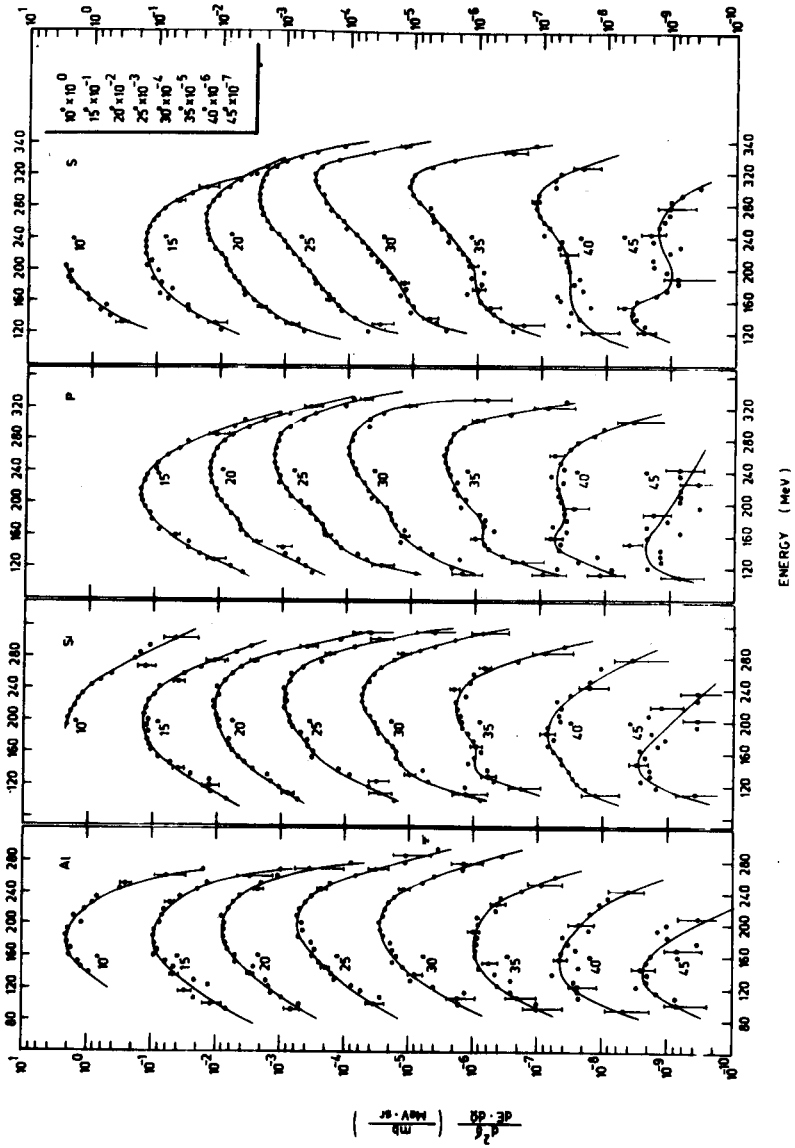

Fig. 4. See caption to Fig. 3.

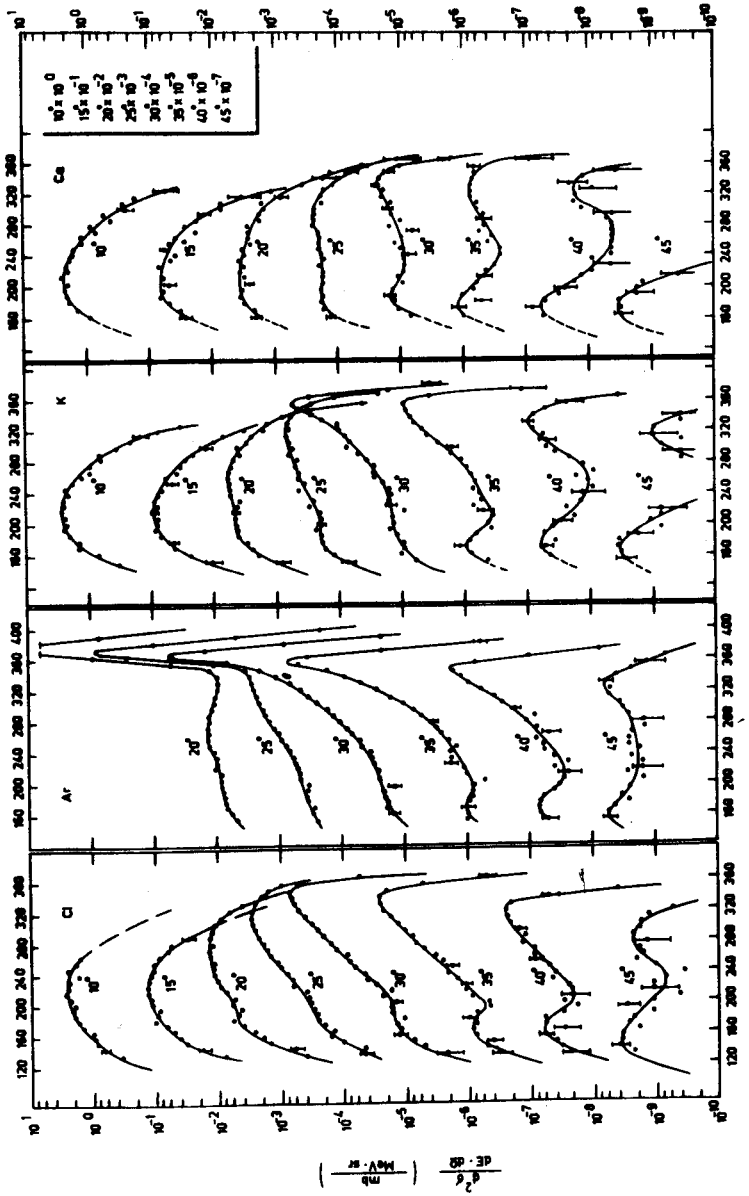

Fig. 5. See caption to Fig. 3.

with ^{22}Ne ions of 174 MeV and ^{40}Ar ions of 290 MeV show that the widths of the element and isotope spectra are close [5,14]. Thus, one may consider that the energy spread introduced into the element energy spectrum by summing up the spectra of separate isotopes is considerably smaller than the dynamic dispersion of the product energy due to the mechanism of interaction of two nuclei in direct reactions.

The energy spectra of the products in multi-nucleon transfer reactions usually have an approximately bell-shaped form. With the lowering of the number of transferred protons, the maxima in the energy spectra are shifted towards higher energies, while the spectra themselves become more asymmetric.

The energy of incident particles greatly affects the widths and shapes of energy spectra. Thus, in icreasing energy from 288 to 379 MeV the FWHM for Mg are changed from 40-50 MeV to 80-90 MeV. The effect of incident particle energy on the shape of the energy spectra is shown in Fig. 6 where the P, Cl and K energy spectra are compared for various detection angles and the incident particle energies. The arrows in Fig. 6 indicate the energy of the light products in the lab. system calculated under the assumption that the nuclear system decay into two products occurs at the zero kinetic energy of relative motion (i.e. corresponding to the Coulomb barrier height for spherical nuclei). It should be noted that if we take into account the velocity of the centre of mass the low energy cut-offs of the spectra for the two incident energies are really equal.

At the ^{40}Ar energy of $E_0 = 379$ MeV the spectra of products of few-nucleon transfer reactions at the angles of 35^0 - 45^0 show two broad peaks one at a low-energy and the other at a high energy (Fig. 5). For $E_0 = 288$ MeV such a spectra separation into two parts at large angles is observed for K and Ca only (Fig. 2).

In general, for few-nucleon transfer reactions, the energy spectra of products tend to become softer with decreasing angle of emission.

3.2. Angular Distribution

The differential cross sections $d\sigma(\theta)/d\Omega$ of light product formation for two values of ^{40}Ar ion energy are shown in Fig. 7. The cross sections have been obtained by integrating the energy spectra $d^2\sigma(\theta, E)/dE \cdot d\Omega$ over energy. Neutron transfer channels and ^{40}Ar inelastic scattering were separated by subtracting the normalized elastic scattering peak for small

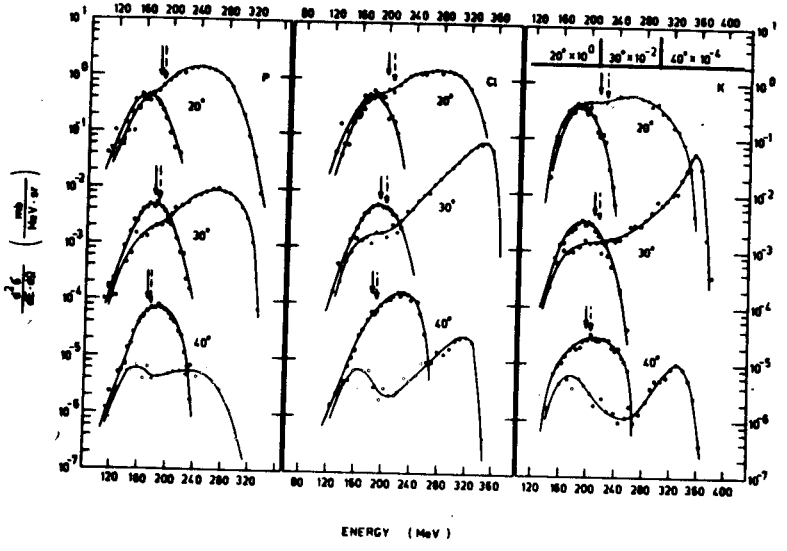

Fig. 6. The dependence of the energy spectrum of the light product on the incident ion energy. The opened circles are the ^{40}Ar energy E = 388 MeV, the filled ones are E = 297 MeV. All the curves and points for each detection angle are multiplied by the coefficients shown in the top right-hand side of the figure. The arrows show product energies for the system decaying into two spherical nuclei from the Coulomb barrier height. The dashed arrow is drawn for the ^{40}Ar energy E = 388 MeV, the solid arrow is drawn for E = 297 MeV.

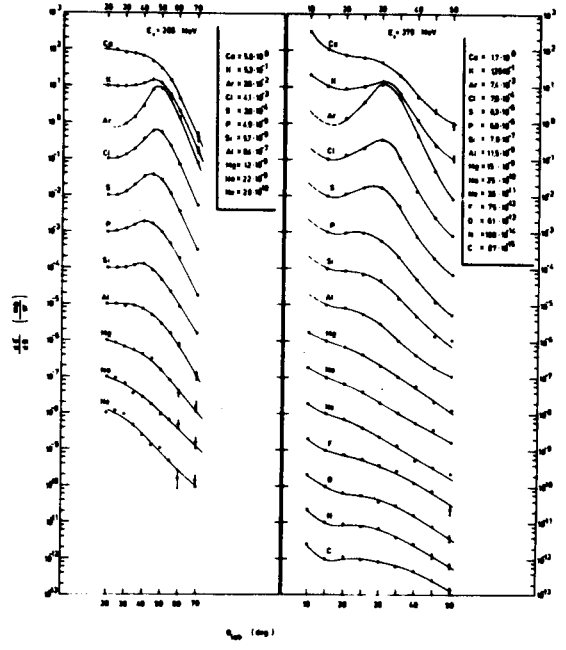

Fig. 7. The laboratory angular distrbutions of light products for ^{40}Ar ion energies in the middle plane of the target E_0 = 288 MeV and E_0 = 379 MeV. Solid curves are drawn through the experimental points. All the points and curves for each element have been multiplied by the coefficients shown in the figure.

angles (10-15^0) from the Ar energy spectrum at an angle θ. Only a part of the spectrum, located 10 MeV below the calculated maximum of the elastic peak at E_0 = 288 MeV and 7 MeV below at E_0 = 379 MeV, was safely separated over the whole angular range. It is this part of the spectrum that was integrated when obtaining Ar angular distribution. Note that in such a treatment the contribution of the Coulomb excitation to the cross section is practically excluded /16/.

As is seen from Fig. 7 the shape of angular distributions varies, in a regular fashion, with the number of nucleons transferred. The peculiar peaks at somewhat smaller angles than that of the ^{40}Ar Rutherford scattering in the grazing collision is clearly seen only for few-nucleon transfer reactions. (The angles of the ^{40}Ar Rutherford scattering in the lab. coordinate system are 55^0 and 36^0, for E_0 = 288 MeV and E_0 = 379 MeV, respectively, and $r_0 = 1.46 \times 10^{-13}$ cm).

With increasing the number of transferred nucleons the width of these peaks of the angular distributions increases, while its maximum is shifted towards smaller angles. In multinucleon transfer reactions the differential cross sections of products increase monotonically with decreasing the emission angle. For the reactions with the transfer of the maximum number of nucleons investigated here (C, N, O for E_0 = 379 MeV) one observes some increase of product yields at larger detection angles. The increase of cross section of an angle of 10^0 for C, N, O, Ca requires a more detailed study since it can be connected with the background effects, e.g., of C and O admixtures in the target.

In earlier investigations /6,8,17/ on the angular distributions of the products of transfer reactions on heavy nuclei both these features of maxima at the Rutherford scattering angles and of monotonously increasing yield towards 0^0 have been obtained. However, only a small number of reaction channels has been detected in the above studies. So it was difficult to determine a definite dependence of the angular distribution shape upon the number of transferred nucleons. The data shown in Fig. 7 with the transfer up to three tens of nucleons, allow to follow the evolution of the angular distribution shape with the increase in the number of transferred nucleons. A similar result for the angular distributions of direct reaction products (light elements from Li to Mg) was obtained by the authors /14/ in the bombardment of ^{232}Th with ^{22}Ne ions.

3.3. Light Product Formation Cross Sections and Total Direct Cross Sections

The cross sections for the formation of light products in direct reactions are shown in Table 1. For each ^{40}Ar energy two values of cross section are given: σ_{meas} and σ. The values of $\sigma_{meas.}$ have been obtained by integrating the differential cross sections $d\sigma(\theta)/d\Omega$ over the angle θ in the angular region where the measurements have been made. These angular intervals were determined using the solid curves drawn through the experimental points as shown in Fig. 7. The values of σ were obtained by integrating the total angular distributions extrapolated to the region of small angles. The total cross sections of direct reactions for the $^{232}Th + ^{40}Ar$ were calculated from our data of the cross section for the formation of separate elements. These values should be considered as the lower limits of the total cross sections of direct processes. The character of the dependence of light product formation cross section on Z allows to assume that the contribution to the total cross sections from elements with charges Z larger and smaller than those shown in Table 1 will be small. The total cross section is somewhat underestimated mainly due to the cutting-off of the Ar energy spectra.

4. Discussion of Experimental Results

4.1. Energy Spectra

In order to clear out the specific features of direct reactions with Ar ions it is useful to compare the kinetic energies of final products with the output Coulomb barrier height. Fig. 8 shows $(E^{in}_{cm} + Q_m - B^{out}_{cm})$ versus the angle of emission of the light products (c.m.s.). Here E^{in}_{cm} is the initial kinetic energy, B^{out}_{cm} is the output Coulomb barrier height (calculated for spherical nuclei having r_0 = 1.46 fm), Q_m is Q-value of the reaction for the maximum product yield. The values B^{out}_{cm} and Q_m were calculated under the assumption of the two-body reaction and for the above isotopes. Note that these values are weakly dependent on the variations of the mass number A.

For few-nucleon transfers the curves $(E^{in}_{cm} + Q_m - B^{out}_{cm})$ have their maxima at angles somewhat smaller than the Rutherford scattering angle of ^{40}Ar (θ^{cm}_{Ruth} = 63^0 for E_0 = 288 MeV and θ^{cm}_{Ruth} = 41^0 for E_0 = 379 MeV). At these angles the kinetic

Table 1
Cross section of light product formation (in mb) in the $^{232}Th + ^{40}Ar$ (297 and 388 MeV) reactions

Energy ^{40}Ar E (MeV)	Product	B	C	N	O	F	Ne	Na	Mg	Al	Si	P	S	Cl	Ar[a]	K	Ca	$\sum Z_i$
297	$\sigma_{meas.}$						3.8	4.4	8.9	18	39	65	150	220	390	52	24	970
	σ						8	9	16	25	50	78	170	240	410	65	38	1100
388	$\sigma_{meas.}$	10	16	11	13	11	18	24	41	46	78	110	210	750	650	110	48	1700
	σ	18	27	19	26	21	33	43	65	86	150	190	300	380	750	140	140	2400

a) *Ar* yield has been determined by using a part of the energy spectrum, see Section 3.2 of the text.

energy of final products is close to E_{cm}^{in} and the process determining the high energy maximum in the energy spectrum is of quasi-elastic character. With decreasing the angle a sharp decrease in the maximum of the final kinetic energy spectrum takes place. It is reduced down to the value close to the height of the output Coulomb barrier, and is further weakly decreased with decreasing θ.

The low energy maxima in the final kinetic energy spectra of products turn out to be lower than the output Coulomb barrier height and are smoothly decreased with increasing angle θ.

T.Kammuri /18/ when calculating the classical deflection of a heavy ion in the Coulomb and nuclear potentials has obtained a possible ion trajectory in traversing 0^0 with respect to the direction of the incident ion. In our case this suggest that the low energy maxima in the spectra of ions emitted at angles of 10^0 to 60^0 are indeed those emitted at angles of -10^0 to -60^0. The points thus plotted are indicated by dashed lines in Fig. 8 which shows that it is possible to connect both the low and high energy maxima in the energy spectra in one system.

For the multi-nucleon transfer reactions the kinetic energy of final products is somewhat smaller than the output Coulomb barrier height for spherical nuclei and varies smoothly with the angle θ. Note the similarity of the positions and the shapes of curves shown in Fig. 8 for the utmost multi-nucleon transfers *(O, F, Ne)* and for the low energy maxima of *Cl, K, Ca*. This fact may be considered as an indication that in both cases we may have the product trajectories with traversing through 0^0.

It is interesting that in some cases the energy spectrum maximum of a light product is below the output Coulomb barrier height (see Figs. 6 and 8). Earlier the production of transfer reaction products at energies below the Coulomb barrier height has been observed on light and medium nuclei /19,20/. One can indicate some possible reasons for the formation of light products with such low energies: 1) the detected product is produced as a result of the decay of a deformed system with relatively smaller values of B_{cm}^{out}, 2) the system decays into more than 2 fragments, of comparable charge and mass, 3) the emission, by the excited light product, of alpha-particles and nucleons in the direction of motion. However, it is improbable that such a process as the decay of the system into more than 2 massive fragments determines the position of maxima in the energy spectra. This is confirmed by the observation of the maxima of the energy spectra being near the Coulomb barrier for two particles in the outgoing channel and furthermore the

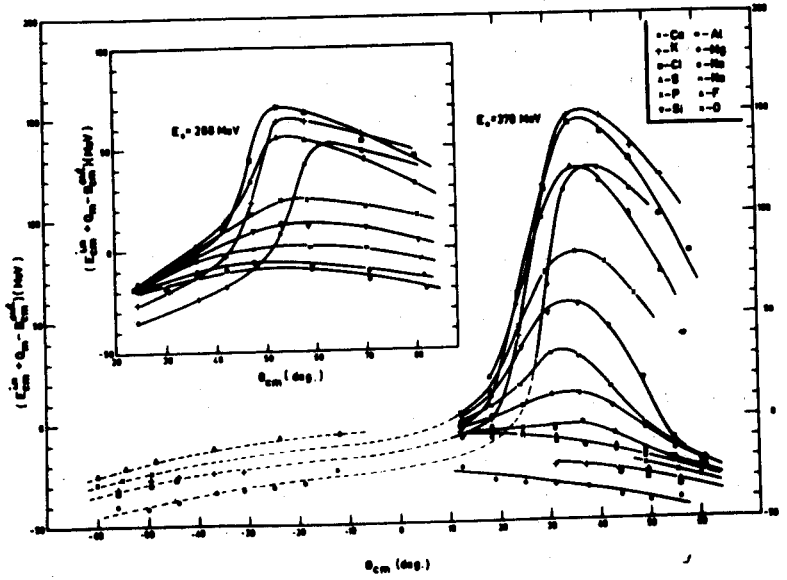

Fig. 8. The difference of kinetic energies in the maximum energy distributions and Coulomb barrier heights of the final products with respect to the light product emission angle. ^{40}Ar ion energies in the middle plane of the target E_0 = 288 MeV and E_0 = 379 MeV.

noticeable limitation of the energy spectra at relatively high energies.

There are no special arguments against the isotropic emission of nucleons or, which is more probable, of alpha-particles by a light product (after the decay of the system). With the isotropic decay of the light product the maximum in the energy spectrum will be determined by alpha-emission in the direction perpendicular to that of product motion. In this case the detection angle for a new product is changed slightly due to its great velocity. (The product energy in system decaying from the Coulomb barrier height is 4-5 MeV/nucleon). At the same time, considering that the velocity of light product after its decay is on an average retained, the variation of the kinetic energy of a new product with respect to the new Coulomb barrier is small. Indeed the points for O, F, Ne in Fig. 8 are practically at the same curve. Thus, one may consider that at the moment of decay of the system, the nuclei are somewhat deformed and the deformation increases with the increase in the angle of the trajectory away from 0^0 .

It is interesting to note that the product yield in such processes is changed slightly over a wide range of atomic number $8 \leq Z \leq 20$ (see product yields in Figs. 3,4,5 for the detection angle of 45^0 where such processes are separated sufficiently well).

4.2. Angular Distributions

In investigations /21,22/ it has been shown that the shape of angular distributions of light products in transfer reactions can significantly change for the different parts of the energy spectrum. In this case the energy spectrum was separated into two parts and for each of them its own angular distribution was determined. Taking into account the large width of energy spectra it is reasonable in our case to consider the angular distribution of reaction products at various excitation energies of the interacting system of two nuclei. Figures 9 and 10 show the differential cross sections for the formation of reaction products as $d^2\sigma/dQ \cdot d\Omega$ with the different Q-values, Q^*. The calculation was made under the assumption of the two-particles in the outgoing channel. As is seen from these Figures, in few-nucleon transfer reactions at small excitation energies of the final nuclei $E^*(E^* = Q_{gg} - Q^*)$ the angular distribution has a pronounced maximum. With increasing excitation energy, the maximum in the angular distribution is shifted towards smaller angles, its width is increased, and a raise of the cross

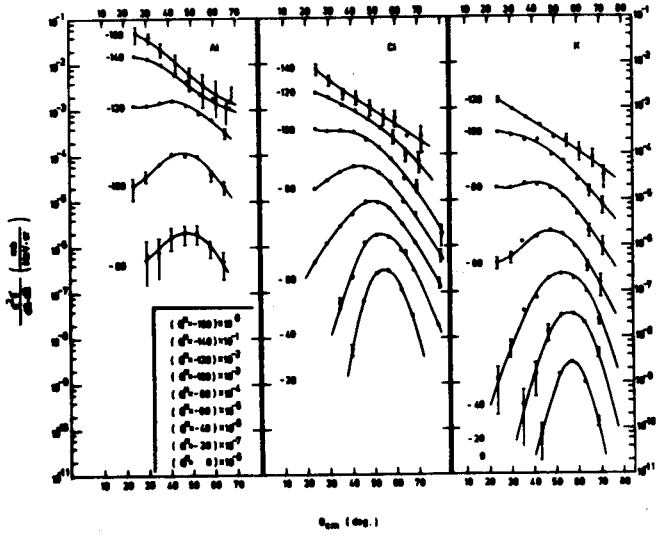

Fig. 9. Partial angular distributions of light products with the fixed value of $Q = Q^*$. ^{40}Ar ion energy $E_0 = 288$ MeV. The curves for K with $Q^* = 0$ MeV and $Q^* = -20$ MeV have been calculated according to Strutinsky /22/. Calculation parameters are presented in Table 2. The remaining curves have been drawn through the experimental points. All the points and curves for the given value of Q^* have been multiplied by the coefficients given in the left-hand side of the figure.

section at small angles appears. At higher excitation energies the yield of products monotonously increases towards 0^0. The radius parameter r_0 calculated (for the closest approach of two nuclei) from the maximum positions in the angular distributions Cl and K with the minimum values of $|Q^*|$ is between (1.55-1.62)x x10^{-13} cm.

Some investigations /18,23-27/ have been devoted to the theoretical analysis of the angular distributions of direct reaction products. Strutinsky's model /24/ is most convenient for comparison with the experimental data. We have calculated the product angular distributions under the assumptions of the ''tangent'' nuclear collisions and the quasi-elasticity of reactions. The function η_ℓ determining reaction intensity in the channel with orbital momentum ℓ has a maximum with some $\ell \simeq \ell_0$ corresponding to the ''tangent'' trajectory. Taking

$$\eta_\ell = \eta_{\ell_0} \cdot q(\ell - \ell_0) = \eta_{\ell_0} \cdot q(x) \qquad (1)$$

two expressions for the function $q(x)$ were considered

$$q(x) = \exp(-\alpha^2 x^2) \qquad (G), \qquad (2)$$

$$q(x) = \begin{cases} \exp(-\alpha x) & \ell > \ell_0 \\ 0 & \ell < \ell_0 \end{cases} \qquad (E). \qquad (3)$$

The quantity $\alpha = 1/\Delta\ell$ determined the wave packet width.

It has been shown that the shape of the angular distribution for light reaction products depends on the number of partial waves giving a contribution to the reaction and the classical deflection angle θ_{max}. The maximum at the angle θ_{max} appears only with the condition $\theta_{max}\Delta\ell^* > 2$. Such an approach allows the extraction of the values $\Delta\ell$ and θ_{max} from the experimentally determined angular distributions.

Table 2 presents the results of calculations of wave packet widths for partial angular distributions of K with $Q^* = 0$ MeV and $Q^* = -20$ MeV. (Here the initial conditions of the model hold). The calculated curves (variant (G)) are shown in Figs. 9, 10. The theoretical curves were normalized to the experimental cross sections at the angles θ_{max}. The agreement of the theoretical curves with the experimental points is quite satisfactory.

In his new investigation V.Strutinsky has generalized his approach for inelastic direct processes /27/. In this variant

Table 2

The analysis of the angular distribution of the light product in the ^{232}Th (^{40}Ar,K) reaction by using the Strutinsky model[27]

Energy ^{40}Ar E_0 (MeV)	Q* MeV	Calculation variant	ϑ_{max} (degrees)	$\Delta\ell$ number of partial waves
288	0	G	57	12
	-20	G	56	9.2
379	0	G	36.5	25.1
	-20	G	35.5	19.4
	-200	E	5	6.3

of the model the angular distribution of reaction products is determined by two factors: by quantum-mechanical dispersion due to the wave nature of the particle and by the dynamic angular dispersion due to nuclear interaction. The mathematical expressions for the angular distributions obtained here are equivalent to expressions of ref.[24]. But since the dynamic dispersion of a packet was not taken into account in the previous paper the parameter $\Delta\ell$ obtained from the analysis of the experimental angular distribution can be smaller than the real width of the wave packet.

However, it is impossible to distinguish the quantum-mechanical and dynamic dispersions within the framework of the proposed model[27]. We have made at attempt to compare the partial angular distributions shown in Figs. 9 and 10 to those calculated using the formulas of the previous work[24]. It was found that for the largest $|Q^*|$ values with $E_0 = 379$ MeV the calculated angular distribution is consistent with the experimental, if the (E) variant is used. Figure 10 shows the corresponding calculated curve for K with $Q^* = -200$ MeV. The calculated parameters are listed in Table 2.

An attempt to fit the theoretical and experimental points for the intermediate values of Q^* using only the Gaussian or the exponent dependence of $q(x)$ has failed. Thus, for comparatively small $|Q^*|$ the character of the decrease in the angular distribution at the angles of $\theta > \theta_{max}$ requires definitely the application of (G), but then the observed increase of cross section at smaller angles can not be explained on this basis. Perhaps it may be possible to explain the observed angular distributions by introducing a varying asymmetry in $q(x)$, from (G) to (E), with increasing excitation energy.

4.3. Direct Reaction Total Cross Section and the Critical Angular Momentum

The comparison of our data for the total cross section of direct reactions σ (See Table 1) with the cross section for incomplete fusion σ_{ICF} obtained by the fission-fragment angular correlation experiments[28] shows a noticeable divergence. The value σ in our experiments turned out to be considerably greater. It is possible that this divergence is due to the difficulties of separation, by the fission-fragment angular correlation method of the complete fusion processes and deep inelastic direct processes with large momentum transfers to the target nucleus.

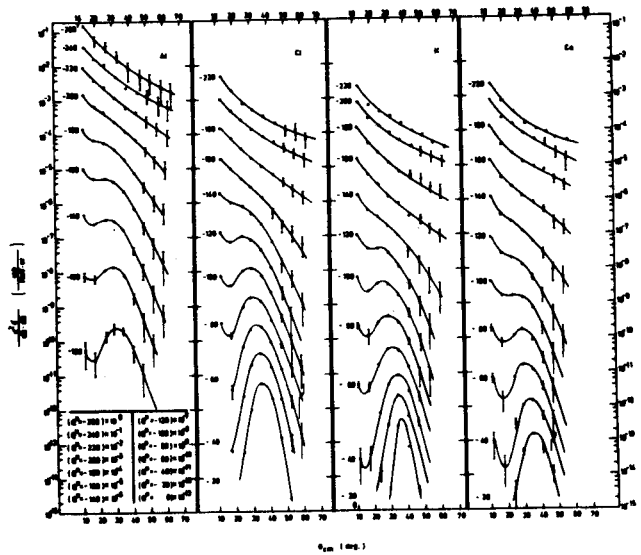

Fig. 10. Partial angular distributions of light products with the fixed value of $Q = Q^*$, ^{40}Ar ion energy $E_0 = 379$ MeV. Curves for K with $Q^* = 0$, Q^* -20 MeV and Q^* = -200 MeV have been calculated according to Strutinsky /22/. Calculation parameters are presented in Table 2. The remaining curves are drawn through experimental points. All the points and curves for the given value of Q^* have been multiplied by the coefficients shown in the bottom left-side of the figure.

The data obtained allow a determination of the value of the critical angular momentum J_{cr} for the $^{232}Th + ^{40}Ar$ system. Natovitz /29/ has remarked that the value $J_{cr} = 170 \cdot \hbar$ obtained from the data of Sikkeland /28/ may have been overestimated. In order to evaluate J_{cr} we have used the same formulas as in /29/:

$$J_{cr} = \left(\frac{\sigma_R - \sigma_{ICF}}{\sigma_R} \right)^{1/2} J_{max}, \quad (4)$$

$$\sigma_R = \pi R^2 \left(1 - \frac{B}{E_{cm}}\right), \quad (5)$$

$$J_{max}^2 = \frac{2\mu (E_{cm} - B) R^2}{\hbar^2}. \quad (6)$$

Here σ_R is the total reaction cross section, σ_{ICF} is the cross section for incomplete fusion, B is the input Coulomb barrier height, μ is the reduced mass, R is the sum of the target and projectile radii ($r_0 = 1.46$ fm), J_{max} is the maximum orbital angular momentum under the assumption of spherical nuclei with sharp boundaries. The results of calculation of J_{cr} are presented in Table 3. The values J_{cr} should be considered as the upper limit for the critical angular momentum, since the limiting value for σ_{ICF} was used in the calculations.

It should be noted that our data for J_{cr} values fit rather well the empirical systematics for critical angular momenta proposed by Natovitz /29/.

5. Conclusion

The results obtained in this experiment demonstrate the possibility of the "element" approach in studying nuclear reactions with the very heavy ions.

Transfer reactions with ^{40}Ar have been shown to occur both in the form of quasi-ealstic and deep inelastic processes. The former are characteristic of few-nucleon transfer reactions. In this case the reaction product retains a major part of the incident ion velocity, whereas the product angular distribution has a pronounced peak at angles close to the Rutherford scattering angle for the incident ion. Deep inelastic processes make a noticeable contribution to few-nucleon transfer reactions and are dominant in multi-nucleon reactions. In such processes all the kinetic energy of nuclear collisions is spent in the rearran-

Table 3
Calculation of the critical angular momentum value of the $^{232}Th + ^{40}Ar$ system according to Natovitz [27]

Energy ^{40}Ar E_0 (MeV)	σ_R (barn)	σ_{ICF} (barn)	J_{max} (units of $\hbar$)	J_{cr} (units of $\hbar$) [a]
288	1.9	1.1	157	102
379	2.9	2.4	222	94

[a] J_{cr} - the upper limit for the critical angular momentum value

gement and excitation of nuclei. The angular distributions are described by a monotonous increase of the yield with decreasing the detection angle.

Such processes are an intermediate stage to the production of the compound-system. This may be suggested by the transition of the trajectory of light product through 0^0 and deformed configuration of the system at the moment of scission.

The transfers of a considerable number of nucleons from a heavy ion to the target nucleus with a noticeable cross section indicate the possibility of using such processes for the synthesis of transuranium elements and, possibly, of superheavy nuclei in a new region of stability. It is worth noting that the large width of the energy spectra of light products increases the probability of processes resulting in the weak excitation of the final heavy products.

The authors are deeply indebted to Academician G.N.Flerov for his interest to this investigation and valuable discussions and to B.A.Zager and the cyclotron operation staff for their cooperation.

References

1. Yu.Ts.Oganessian, Yu.E.Penionzhkevich and O.A.Shamsutdinov. Yad.Fiz., 14, 54 (1971).
2. A.G.Demin, V.Kusch, M.B.Miller, A.S.Pasyuk, A.A.Pleve, Yu.P.Tretiakov. Proc. of the Int. Conf. on Heavy Ion Physics. Dubna, 11-17 Febr. 1971; JINR, D7-5769, Dubna, 1971, p. 169.
3. R.Bimbot, C.Deprun, H.Gauvin, Y.L.Beyec, M.Lefort, J.Peter, B.Tamain. Nature, 234, 215 (1972).
4. G.N.Flerov, Yu.Ts.Oganessian. JINR Preprint, P7-6523, Dubna, 1972.
5. A.G.Artukh, V.V.Avdeichikov, G.F.Gridnev, V.L.Mikheev, V.V.Volkov, J.Wilczynski. Nucl. Phys., A176, 284 (1971).
6. H.Kumpf, E.D.Donets. JETP (Sov.Phys.)., 17, 539 (1963).
7. W.Grochulski, T.Kwiecinska, Lian Go-chan, E.Lozynski, J.Maly, L.K.Tarasov, V.V.Volkov. Proc. Third Conf. on Reactions between Complex Nuclei, ed. A.Chiorso, R.M.Diamond, H.E.Conzett (University of California Press, Berkeley, 1963), p. 120.
8. E.Lozynski, I.I.Chuburkova. JINR Preprint, P7-3630, Dubna, 1967.
9. A.G.Artukh, V.V.Avdeichikov, J.Ero, G.F.Gridnev, V.L.Mikheev, V.V.Volkov. Nucl.Instr. and Meth., 83, 72 (1970).
10. M.W.Sachs, C.Chasman, D.A.Bromley. Nucl.Instr. and Meth., 41, 213 (1966).
11. G.W.Butler, A.M.Poskanzer, D.A.Landis. Nucl. Instr. and Meth., 89, 189 (1970).
12. A.G.Artukh, V.V.Volkov, L.Pomorski, J.Tys. JINR Preprint, P7-5494, Dubna, 1970.

13. L.C.Nortcliffe, R.F.Schilling. Nucl.Data Tables, A7, 233 (1970).
14. A.G.Artukh, J.Wilczynski, V.V.Volkov, G.F.Gridnev, V.L.Mikheev. JINR Preprint, P7-6815, Dubna, 1973.
15. S.A.Karamjan, Yu.Ts.Oganessian, Yu.E.Penionzhkevich, B.J.Pustilnik. JINR Preprint, P7-5884, Dubna, 1971.
16. K.Alder, A.Bohr, T.Huns, B.Mottelson, A.Winter. Rev.Mod. Phys., 28, 432 (1956).
17. E.Lozunski. JINR Preprint, P-1486, Dubna, 1963.
18. T.Kammuri. Prog.Theor.Phys., 28, 934 (1962).
19. J.Wilczynski, V.V.Volkov, P.Decowski. Yad.Fiz., 5, 942 (1967).
20. G.F.Gridnev, V.V.Volkov, J.Wilczynski. Nucl.Phys., A142, 385 (1970).
21. A.G.Artukh, G.F.Gridnev, V.L.Mikheev, J.Wilczynski, V.V.Volkov. Proc. of the Int. Conf. on Nuclear Reaction Induced by Heavy Ions, edited by R.Bock and W.R.Hering (North-Holland, Amsterdam-London, 1970), p. 140.
22. J.Galin, D.Guerreay, M.Lefort, J.Peter, X.Tarrago, R.Rasile, Nucl.Phys., A159, 461 (1970).
23. B.N.Kalinkin, J.Grabowski. Proc. Third Conf. on Reactions between Complex Nuclei, Asilomar, 1963 (Univ. Calif. Press, 1963), p. 129.
24. V.M.Strutinsky. ZhETF (USSR), 46, 2078 (1964).
25. W.E.Frahn, R.H.Venter. Nucl.Phys., 59, 651 (1964).
26. R. da Silveira. Communications European Conf. on Nucl. Physics. Aix-en-Provence (France), 1972 (Comptes Rendus, 1972), p. 57.
27. V.M.Strutinsky. Nucl.Phys. (To be published).
28. T.Sikkeland. UCRL-16580 (1965).
29. J.B.Natovitz. Phys.Rev., 1C, 623 (1970).

Received by Publishing Department
on February 27, 1973.